The Journal of Chemical Physics

Size and temperature dependence of photoluminescence of hybrid perovskite nanocrystals

Cite as: J. Chem. Phys. **151**, 154705 (2019); https://doi.org/10.1063/1.5124025
Submitted: 12 August 2019 . Accepted: 28 September 2019 . Published Online: 21 October 2019

Sara Bonabi Naghadeh, Som Sarang, Amanda Brewer, A'Lester Allen, Yi-Hsuan Chiu, Yung-Jung Hsu, Jhen-Yang Wu, Sayantani Ghosh, and Jin Z. Zhang

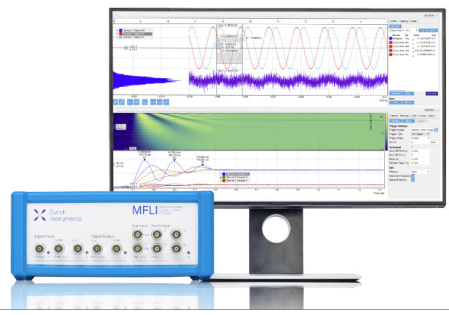

The Journal of Chemical Physics ARTICLE scitation.org/journal/jcp

Size and temperature dependence of photoluminescence of hybrid perovskite nanocrystals

Cite as: J. Chem. Phys. 151, 154705 (2019); doi: 10.1063/1.5124025
Submitted: 12 August 2019 • Accepted: 28 September 2019 •
Published Online: 21 October 2019

Sara Bonabi Naghadeh,[1] Som Sarang,[2] Amanda Brewer,[1] A'Lester Allen,[1] Yi-Hsuan Chiu,[3] Yung-Jung Hsu,[3] Jhen-Yang Wu,[3] Sayantani Ghosh,[2,a)] and Jin Z. Zhang[1,a)]

AFFILIATIONS

[1]Department of Chemistry and Biochemistry, University of California, Santa Cruz, California 95064, USA
[2]Department of Physics, School of Natural Sciences, University of California, Merced, California 95340, USA
[3]Department of Materials Science and Engineering, National Chiao Tung University, Hsinchu 30010, Taiwan

Note: This paper is part of the JCP Special Topic on Colloidal Quantum Dots.
[a)]**Authors to whom correspondence should be addressed:** sghosh@ucmerced.edu and zhang@ucsc.edu

ABSTRACT

In this work, we studied the effects of particles' size and temperature on the photoluminescence (PL) of $CH_3NH_3PbBr_3$ perovskite nanocrystals (PNCs), with the PNC size controlled by varying the surface passivating ligands. The structural and optical properties of the PNCs were investigated using UV-Vis and PL spectroscopy, revealing strong quantum confinement effects. Temperature dependent PL measurements showed the spectral blue shift of the PL peak for the small PNCs (3.1 ± 0.2 nm) with decreasing temperature from 300 K to 20 K, which is opposite to the red shift with decreasing temperature observed for large- (9.2 ± 0.5 nm) and middle-sized (5.1 ± 0.3 nm) PNCs. The PL lifetime also increased with increasing temperature for the larger PNCs, while it remained about the same for the small and middle-sized PNCs. This increase in lifetime with temperature is attributed to exciton dissociation to free carriers at higher temperatures and to the formation of polar domains in the PNCs. However, the small and middle-sized PNCs did not show such a trend, which may be due to efficient defect passivation as higher concentration of 3-aminopropyl trimethoxysilane (APTMS) was used and to the role of particle size in surface state delocalization. Cryo-X-ray diffraction showed no new peak formation or peak splitting as temperature was varied, which suggests efficient crystal phase stabilization in PNCs of all three sizes controlled by the concentration of APTMS. These results emphasize the importance of size and surface properties of PNCs in their optical properties such as PL quantum yield, PL lifetime, and crystal phase stability.

I. INTRODUCTION

Organic-inorganic metal halide perovskite in the form of thin films, single crystals, and nanocrystals (NCs) has attracted significant attention in recent years as a potential efficient and flexible alternative for silicon in photovoltaic applications. Perovskite nanomaterials with ABX_3 formula (where A is an organic/inorganic cation, B is a metal cation such as Pb or Sn, and X is a halide anion such as Cl, Br, and I) offer flexibility in composition variation, which can tune their optical and structural properties. In addition, easy and low-cost processing, tunable bandgap, large absorption coefficient, long exciton lifetime, and large charge carrier mobility[1–3] make them outstanding candidates for various applications, such as photovoltaic (PV) solar cells, light-emitting diodes (LEDs), photodetectors, sensors, lasers, and photoelectrochemical cells.[4–8] The successful implementation of perovskite nanomaterials in PV devices inspired researchers to study the fundamental properties of the material, such as intrinsic chemical, thermal, and crystal phase instability, and electronic structure, and to tune their photophysical properties. Specifically, perovskite quantum dots (PQDs) or nanocrystals (PNCs), because of their large surface to volume ratio, tunable bandgap, variation in size and strong absorption/emission quantum yield, are considered as good models to study optical and structural optimization. For example, substituting

methylammonium (MA) with formamidinium (FA) significantly enhanced the chemical stability; however, FA based PNCs showed phase transition to the yellow nonperovskite polymorph (δ-phase), very close to photovoltaic operational temperatures, making device performance unpredictable.[9] In another study, time-resolved measurements show that the radiative lifetime of the band-edge emission depends strongly on the halide ion and increases with temperature.[10] Interestingly, the crystal size of PNCs can also tune their phase diagram, material stability, and photophysical properties.[11] We also recently studied the effect of PNC size and capping ligand concentration on the band structure of $CH_3NH_3PbBr_3$ NCs and revealed the dominant effect of surface properties on nonradiative components of lifetime, while the radiative lifetime was mostly influenced by PNC size.[12]

Although most work with these materials is focused on room-temperature behavior, low-temperature measurements offer the opportunity to answer fundamental questions about the material, including changes in the bandgap, exciton binding energy, and electronic structure. It was previously observed for perovskite thin films that the long recombination lifetime in the tetragonal phase decreased an order of magnitude following the transition to the orthorhombic phase at lower temperatures. The same trend was observed by Sarang *et al.*, which attributed this behavior to the crossover from free carriers to exciton-dominated radiative recombination.[13] On the contrary, Li *et al.* reported a significant PL lifetime increase of inorganic $CsPbBr_3$ NCs by increasing the temperature to 300 K and then a sudden decrease in the lifetime by further increasing the temperature over 300 K, suggesting thermal instability in inorganic PNCs.[14] We also recently found a correlation among surface property, phase transition, and exciton dynamics for $CH_3NH_3PbBr_3$ NCs capped with APTES and OABr at different temperatures.[15] The observation of a higher energy band in the PL spectra indicated a structural phase transition from tetragonal to orthorhombic at 140 K for PNCs capped with OABr. However, PNCs capped with APTES did not show any structural change even at 20 K. This capping ligand-dependent phase transition also resulted in a sudden decrease in recombination lifetimes.[15] These results, demonstrating the effect of surface properties and temperature on the structural and optical properties of the PNCs, motivated us to further extend this work.

Here, we studied the effect of size [by varying the APTMS (3-aminopropyl trimethoxysilane) concentration] and temperature on the photoluminescence of $CH_3NH_3PbBr_3$ PNCs using UV-Vis and photoluminescence (PL) spectroscopy. Temperature dependent static and time-resolved PL (TRPL) revealed an opposite spectral shift with temperature for small PNCs and a significant difference in their recombination lifetime. We further investigate temperature dependent crystal phase transition and concurrent lattice expansion using cryo-X-ray diffraction (XRD) and cryo-EM over the same range as the other measurements for a complete picture.

II. EXPERIMENTAL

A. Materials

All chemicals were used as received without further purification: toluene (spectroscopic grade, Fisher Scientific), *N*,*N*-dimethylformamide (DMF, spectroscopic grade, Fisher Scientific), methylammonium bromide (MABr) (Greatcell Solar Australia Pty Ltd.), lead bromide (98+%, Alfa Aesar), OA (90%, Alfa Aesar), and 3-aminopropyl triethoxysilane (APTMS) (99%, Sigma-Aldrich).

B. Synthesis

A ligand-assisted reprecipitation method was used to synthesize the $CH_3NH_3PbBr_3$ NCs. Briefly, 0.157 mmol of MABr and 0.200 mmol of lead bromide ($PbBr_2$) were dissolved in 400 μl DMF and sonicated until clear. 100 μl of OA and varying amounts of APTMS (20, 35, and 50 μl) were added to separate solutions to control the particle size. The precursor solution was further sonicated to reach a homogeneous solution and then injected into 5 ml toluene to precipitate and collect the nanocrystals. The resultant nanocrystals were centrifuged at 6000 rpm for 5 min and washed with toluene twice to remove unreacted precursors. A portion of the collected precipitate was dried for powder XRD characterization, and the rest was redispersed in toluene for film fabrication. The redispersed solutions were spin-coated on a glass substrate at 4500 rpm to achieve an uniform film for optical characterizations.

C. Instruments and characterization

UV–Vis and fluorescence spectra of the prepared nanocrystal films were collected on Agilent Technologies Cary 60 and FluoroMax-3, respectively. XRD was used to obtain the crystalline phase at a voltage of 40 kV and a current of 30 mA using a Rigaku America Miniflex Plus powder diffractometer. The scanning angle range was 10°–60° (2θ) with a rate of 3° min^{-1}. TEM and HRTEM were carried out to investigate the size, morphology, and lattice spacing of the PNCs. The TEM study was carried out using a FEI UT Tecnai HRTEM microscope operated at a 200 kV accelerating voltage. The PL data were taken using an Acton 300i spectrometer, and the signal was then dispersed onto a thermoelectrically cooled charge-coupled device (CCD) with a spectral resolution of 0.18 nm. For time-resolved PL measurements, we used a time-correlated single-photon counting (TCSPC) system (Picoquant) in conjunction with the pulsed source. The temperature-dependent measurements were done in a cryo-free system from Advanced Research Systems with a base temperature of 10 K. Cryo-XRD was performed using a Bruker D8 discover X-ray diffraction system equipped with a PheniX cryostat with the temperature range of 12–290 K.

III. RESULTS AND DISCUSSION

A. TEM, UV-Vis, and PL spectroscopy

Controlling the particle sizes was achieved using different concentrations of APTMS as a capping ligand in the dissolution–precipitation synthesis method similar to previous reports.[16] The TEM images in Figs. 1(a)–1(c) show the formation of uniform spherical particles, with an average diameter of 9.2 ± 0.5, 5.1 ± 0.3, and 3.1 ± 0.2 nm when 20, 35, and 50 μl of APTMS were used in the synthesis. These samples are labeled PNC_{20_APTMS}, PNC_{35_APTMS}, and PNC_{50_APTMS}, respectively. As shown in TEM images, the size of resultant PNCs was decreased by increasing the APTMS concentration. This trend is due to the coordinating effect of capping

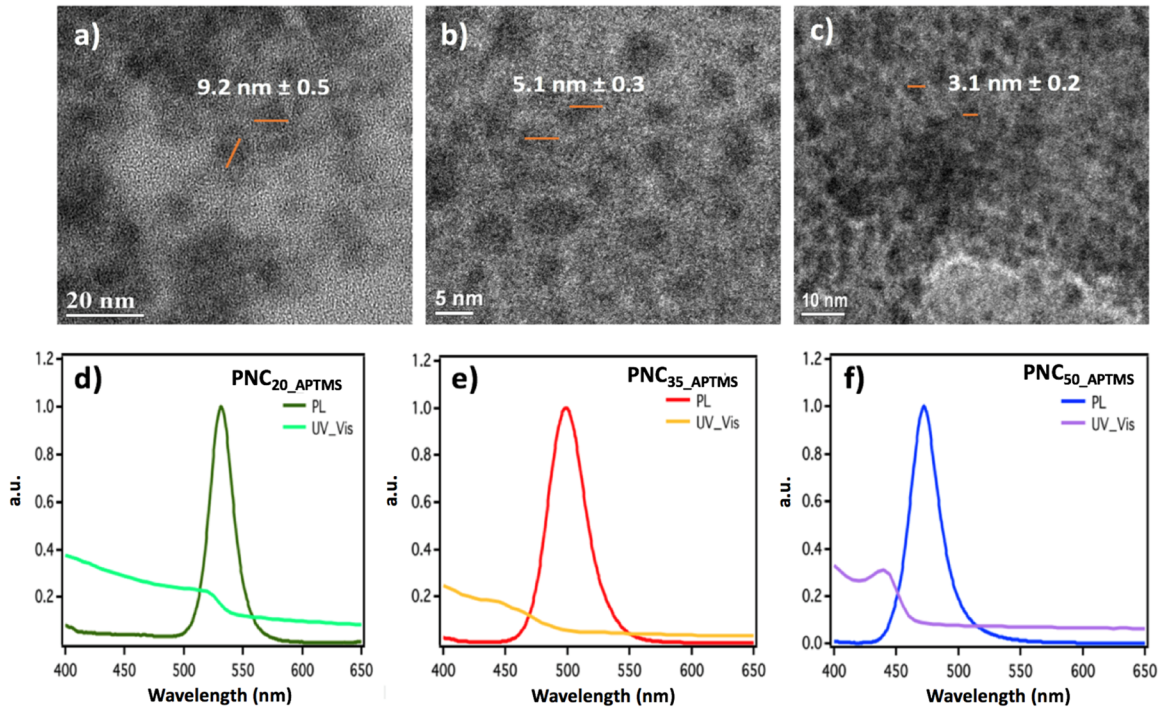

FIG. 1. TEM images of (a) PNC_{20_APTMS}, (b) PNC_{35_APTMS}, and (c) PNC_{50_APTMS}. (d) UV–Vis and PL spectra (λ_{ex} = 360 nm) of PNC_{20_APTMS}, (e) PNC_{35_APTMS}, and (f) PNC_{50_APTMS} spin-coated on the glass substrate at 4500 rpm. The orange solid lines in Figs. 1(a)–1(c) refer to the diameter of PNCs.

ligands which slows down the rate of monomer transfer to the PNC surface and thereby limits growth. Irrespective of sizes, PNCs displayed great uniformity attributed to the strong steric hindrance of branched APTMS ligands, as reported previously.[16]

Using spin coating, each sample was deposited as a thin film on a glass substrate and their optical properties were studied by UV-Vis and PL spectroscopy. As shown in Figs. 1(d)–1(f), the UV–Vis spectra of PNC_{20_APTMS} exhibit an excitonic absorption peak at 520 nm with an extended tail at lower energies due to the scattering from relatively larger particles. However, the absorption onset of PNC_{35_APTMS} and PNC_{50_APTMS} is blue shifted to 490 and 440 nm, respectively. This spectral shift is due to the decrease in PNC size and strong quantum confinement effect in particles with the sizes smaller than the exciton Bohr radius.[17–21] After excitation at 360 nm (λ_{ex}), a similar blue shift was observed for the narrow and symmetric PL emission bands, moving from 530 nm for PNC_{20_APTES} to 470 nm for PNC_{50_APTES}. These narrow emission peaks and the small full width at half-maximum indicate the uniform distribution in particle size, as shown in the TEM images in Figs. 1(d)–1(f). In addition, a larger Stokes shift (~41 meV) was observed as the PNC size decreased from 9.2 to 3.1 nm. This size-dependent Stokes shift has been reported previously for CdSe QDs as well as all-inorganic PNCs such as $CsPbBr_3$.[22] Theoretical calculations have revealed the presence of an inherent, size-dependent confined hole state above the valence band (VB) for $CsPbBr_3$ NCs between the sizes of 2 and 5 nm. This hole state is proposed to be dark in absorption but bright in emission due to its low population density, which explains the size-dependent Stokes shift.[22] Because cesium orbitals do not contribute to this identified confined hole state, this size-dependent Stokes shift can be assumed to be a general feature in other PNCs similar to what we observed here for $CH_3NH_3PbBr_3$ PNCs. In another study, Sercel *et al.* also suggested that the size dependence of the exciton structure is due to bright-dark level inversion caused by the Rashba effect, which is suppressed by the enhance electron-hole exchange interaction in small NCs.[23] The presence of this bright state in $CsPbBr_3$ is further studied by Becker *et al.* which can happen when the strong spin-orbit coupling in the conduction band of perovskite is combined with the Rashba effect.[24]

B. Temperature dependent PL

Figures 2(a)–2(c) show the PL intensity of different sized PNCs as a function of emission wavelength and temperature. As shown in Figs. 2(a) and 2(b), large- and middle-sized PNCs (9.2 nm and 5.1 nm) show a red shift in the PL peak with decreasing temperature from 300 K to 20 K. This is similar to what was reported previously for various PNCs.[15,25,26] In Figs. 2(d) and 2(e), the line cuts of the same maps are represented at 20, 150, and 290 K. It is clearly shown that the PL emission peak of PNC_{20_APTMS} shifted from 530 nm at room temperature (RT) to 552 nm at 20 K. Similarly, for PNC_{35_APTMS}, the spectral peak shifted from 492 nm at RT to 508 nm at 20 K. Generally, in semiconductors, the bandgap energy increases with lowering temperature. This change in band structure with temperature is due to the temperature induced lattice

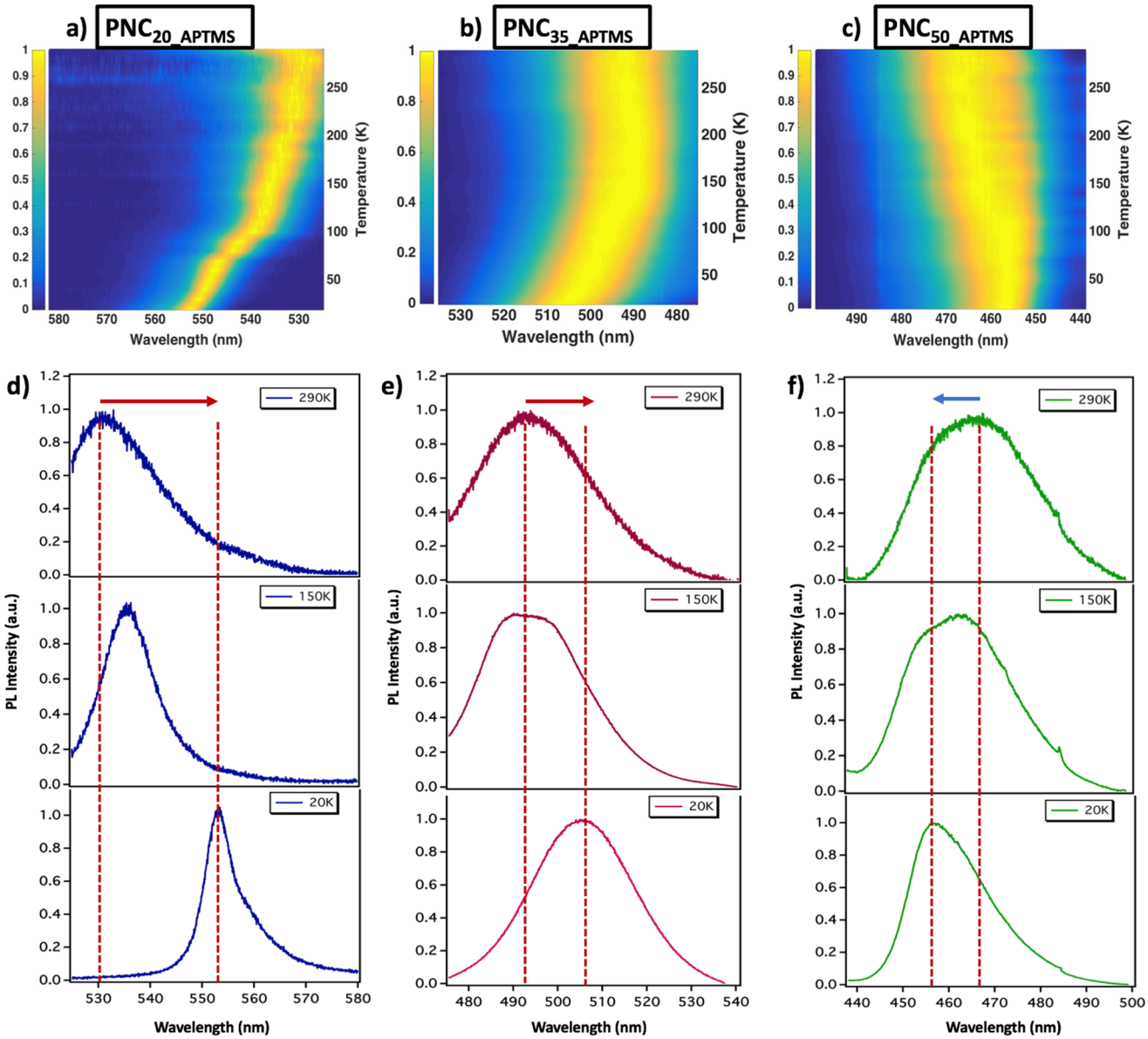

FIG. 2. PL intensity mapped with the emission wavelength and temperature for (top panels) P-OABr and (bottom panels) P-APTMS: (a) PNC_{20_APTMS}, (b) PNC_{35_APTMS}, and (c) PNC_{50_APTMS}. Line cuts of the same maps at 20, 150, and 290 K for (d) PNC_{20_APTMS}, (e) PNC_{35_APTMS}, and (f) PNC_{50_APTMS}.

dilatation and electron–lattice interaction.[27] However, perovskites show an atypical variation of bandgap energy with temperature, which is attributed to their reverse band structure.[25,26,29,30] This may also be related to bright–dark level inversion caused by the Rashba effect that can be suppressed by the enhanced electron–hole exchange interaction in small NCs.[23] In addition to the spectral shift, the full width half maximum (FWHM) decreased significantly with decreasing temperature. This can be simply related to the so-called Varshni effect.[31] The PL spectra, in general, are formed by emission from different localized states at the same time which results in larger FWHM at RT. At higher temperatures (up to 300 K), the thermal activation energy enables the carriers in the lower energy levels to hop and occupy the higher energy levels of the strongly localized states, which leads to the blue shift of the peak energy and the increase of the FWHM.[32] The change in line shape observed for $PNCs_{20\_APTMS}$ and $PNCs_{35\_APTMS}$ at lower temperatures is consistent with lower thermal energy, which reduces homogeneous broadening.[28]

However, the PL spectra of the small PNCs (3.1 nm) showed an opposite trend and slightly blue shifted from 468 nm at 290 K to 458 at 20 K with decreasing temperature. A similar spectral blue shift was reported previously for $CH_3NH_3PbI_3$ and $CH_3NH_3PbBr_3$ perovskite nanomaterials and was attributed to crystal phase change.[25,26,33,34] The spectral shift onset started at ~160 K which is the temperature that was reported as the phase transition region from tetragonal to orthorhombic.[33] In some other studies, it has been shown that this phase change and spectral shift are significantly dependent on the halide type. Saran *et al.* investigated the PL of ($CsPbX_3$, where X is Cl, Br, or I) NC perovskites[35] and reported a wide broadening of the excitonic linewidth in these NCs, which arises from strong exciton–phonon coupling. $CsPbBr_3$ and $CsPbI_3$ NCs displayed a general red shift of their emission energy peaks with decreasing temperature. However, the $CsPbCl_3$ NCs with smaller halides in the structure displayed a blue shift and underwent a structural phase transition at ≈175–200 K. This temperature-dependent blue shift was attributed to a phase change in the crystal structure.[35] However, no higher energy peaks were observed for all three different sized PNCs, suggesting crystal phase stabilization using different concentrations of the branched APTMS capping ligand.

C. Temperature dependent TRPL

To study the effect of size and capping ligand concentration on the charge carrier lifetime as a function of temperature, we measured time-resolved PL as a function of temperature for all three samples (PNC_{20_APTMS}, PNC_{35_APTMS}, and PNC_{50_APTMS}) between 290 and 20 K. The average lifetimes of exciton decay for all PNC_{APTMS} samples were calculated by fitting the data in Fig. 3 to a biexponential fit. The average values of these recombination times, extracted from fits, are plotted in Figs. 3(d)–3(f) for PNC_{20_APTMS}, PNC_{35_APTMS}, and PNC_{50_APTMS}. All PNCs showed an average lifetime of ~2–3 ns. However, even without the benefit of quantitative analysis, a difference between the trends with temperature is clearly visible. For large PNCs (PNC_{20_APTMS}), the time-resolved curves show a continuous and gradual decrease in exciton lifetime with decreasing temperature. Based on previous reports, this reduction in charge carrier lifetime with lowering temperature arises from the interactions of free and trapped excitons with surface states or localized states as relaxation pathways.[14,36–39] These surface or localized states are defects, which can be formed as a result of chemical and structural changes in the material. It has been extensively studied that these defect states are also a detrimental factor impacting device performance as they

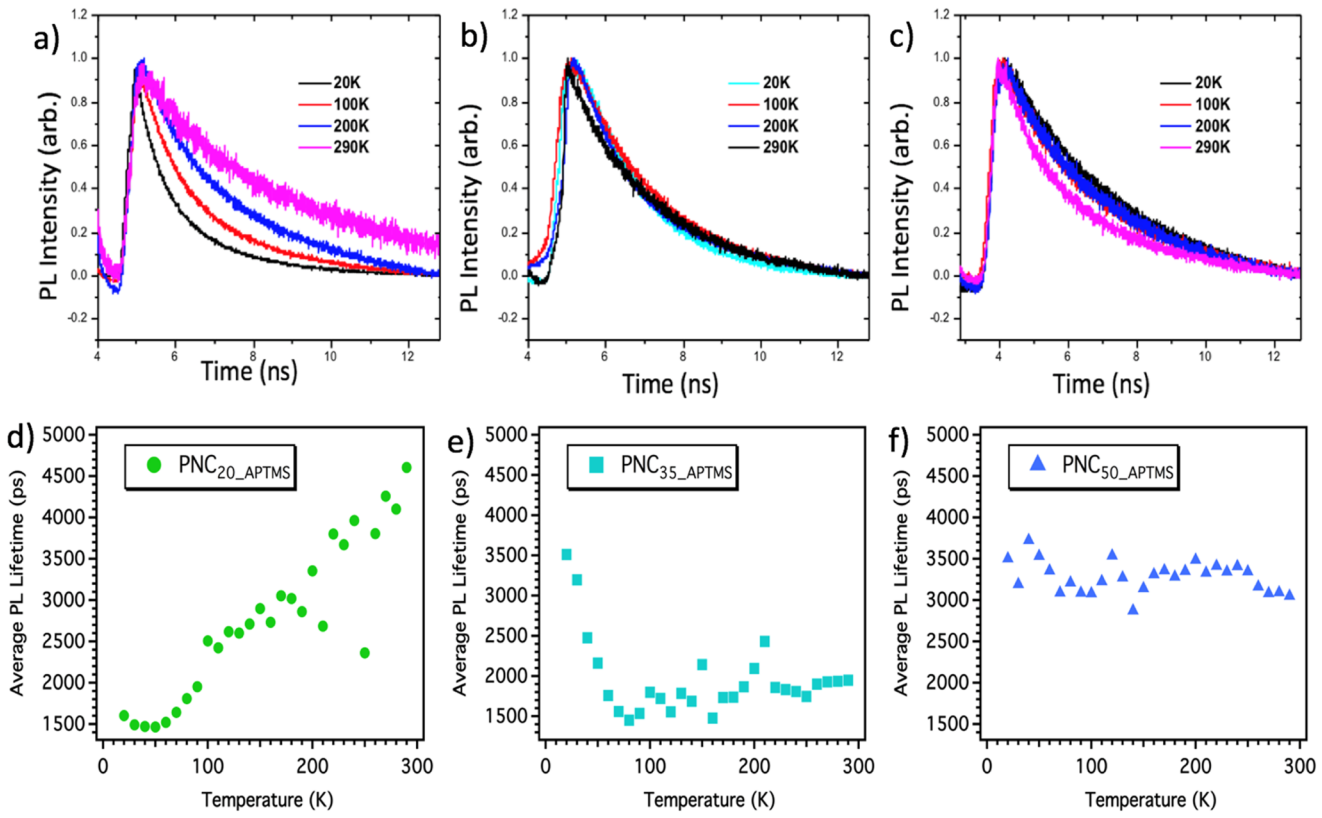

FIG. 3. Time-resolved PL curves for (a) PNC_{20_APTMS}, (b) PNC_{35_APTMS}, and (c) PNC_{50_APTMS} as a function of temperature. Recombination lifetimes extracted from biexponential fits for PNC_{20_APTMS}, PNC_{35_APTMS}, and PNC_{50_APTMS} are plotted in (d), (e), and (f), respectively.

provide recombination channels for photogenerated charge carriers. However, the lifetime of the middle-sized (PNC_{35_APTMS}) and smaller PNCs (PNC_{50_APTMS}) showed reverse behavior compared to large-sized PNCs and did not change noticeably with decreasing temperature. Our group previously studied the effect of APTES concentration on charge carrier dynamics of different sized PNCs, and the results indicated improved passivation of surface defects and localized states when higher concentration of this branched capping ligand was used.[12] Therefore, the proper passivation of these states will result in reduced interaction and trapping of photogenerated exciton and minimal change in PL lifetime, as observed here. In addition, it has been suggested that the formation of polar domains, which are more predominant at higher temperatures, can result in longer PL lifetimes.[10] Similar behavior in PL lifetime was previously observed when $CsPbI_3$, $CsPbBr_3$, and $CsPbCl_3$ were compared.[39] In this study, $CsPbI_3$ demonstrated a significant increase in lifetime, which is attributed to exciton dissociation to free carriers at higher temperatures. Similar to what we observed here, when the size of halide in the $CsPbX_3$ changed from I to Cl, the PL lifetime remained unchanged for a broader range of temperatures. In addition, Diroll *et al.* showed as the NC size increased, the lifetime increased, which suggests that the spatial extent of charge carrier delocalization controlled by the PNC size can play a role in the radiative rate in NCs.[39]

D. Low temperature XRD

In order to understand the reason behind the atypical PL blue shift with lowering temperature, observed in the PNC_{50_APTMS}, and investigate the possibility of phase change in these NCs, cryo-XRD measurements were performed. XRD peaks of all three samples at temperatures ranging from 15 K to 300 K are shown in Figs. 4(a)–4(c).

The XRD patterns shown in Fig. 4 were used to determine the crystal structure of the PNCs. The peaks centered at 14.80°, 21.03°, 29.98°, 33.55°, 36.93°, 42.83°, and 45.69° can be indexed to the cubic phase $CH_3NH_3PbBr_3$ perovskite, indicating sample crystallinity and purity.[40] When the amount of APTMS was increased, significant broadening in XRD peaks was observed because of the presence of smaller PNCs and amorphous silica as a result of higher concentration of APTMS on the samples.[41] Further increasing the APTMS concentration resulted in the formation of the bulk material instead of PNCs. As shown in Figs. 4(d)–4(f), all the peaks shifted toward large diffraction angles as the temperature decreased due to changes in cell parameters caused by lattice contraction.[25] In these cryo-XRD patterns, the absence of new peak or peak splitting overrules the possibility of crystal phase transition to lower energy phases such as orthorhombic or tetragonal for all three sizes of PNCs capped with APTMS. This result confirms the stabilization of the perovskite

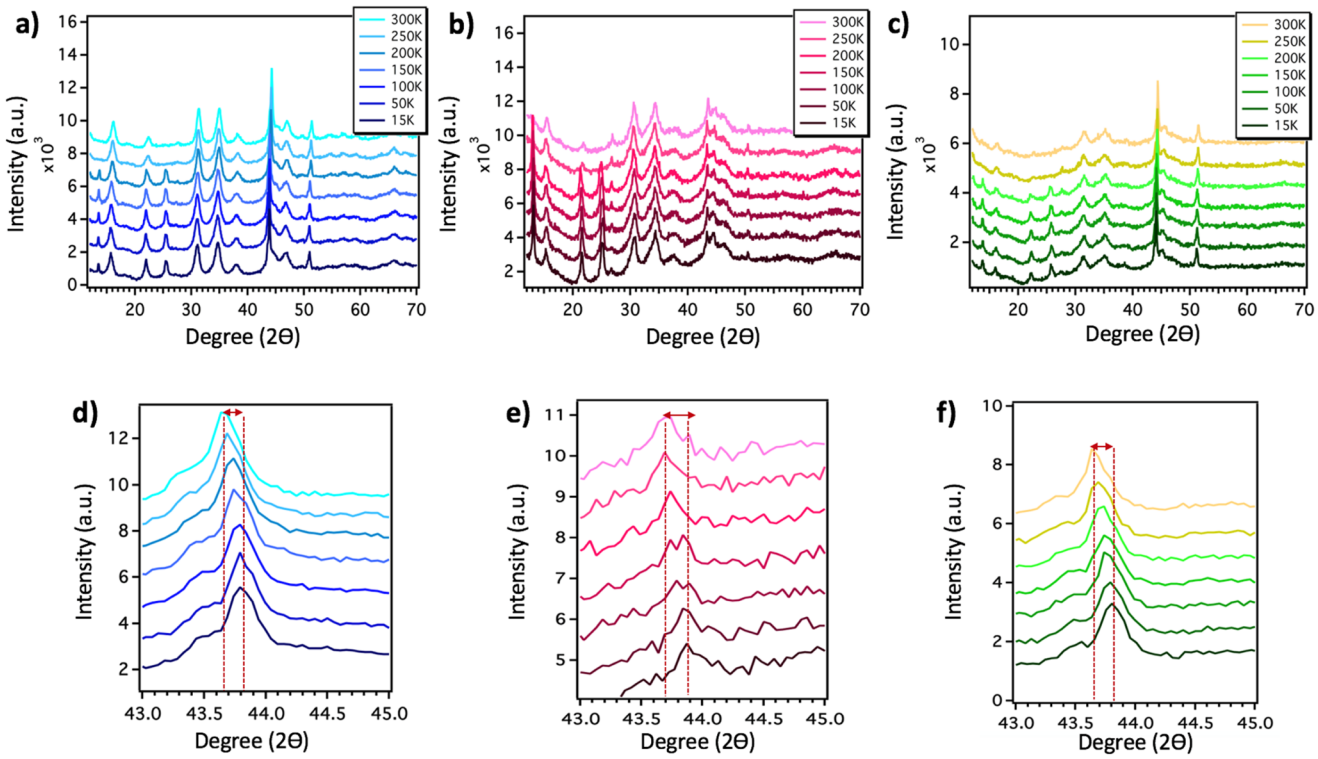

FIG. 4. XRD peaks of (a) PNC_{20_APTMS}, (b) PNC_{35_APTMS}, and (c) PNC_{50_APTMS} at temperatures ranging from 15 K to 300 K. (d) PNC_{20_APTMS}, (e) PNC_{35_APTMS}, and (f) PNC_{50_APTMS} from 43° to 45° are the zoomed-in peaks of (a)–(c), respectively.

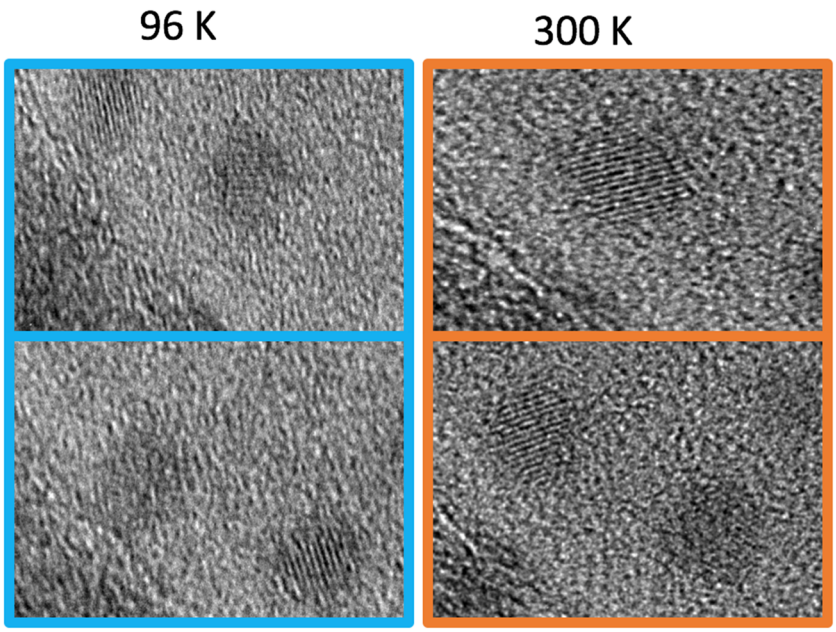

FIG. 5. HR-TEM images of PNC_{35_APTMS} at 96 K and 300 K.

crystal phase using the branched APTMS capping ligand at different concentrations.

E. Cryo-TEM

In order to determine the possible lattice parameter changes with temperature, high resolution TEM images were collected for PNC_{20_APTMS}, PNC_{35_APTMS}, and PNC_{50_APTMS} at 300 K and 96 K. Figure 5 shows the HR-TEM images of PNC_{35_APTMS} at 96 K and 300 K, and the d-spacing in the lattice was measured for six different particles at both temperatures. The resultant d-spacing and the average are reported in Table I. As shown in Table I, aside from small differences, the average d-spacing for the PNCs did not change at different temperatures. This might mostly be due to the rotation of PNCs under the microscope, which is a common phenomenon. This rotation eventually results in inaccurate measurement of the lattice parameters. Even though this lattice contraction and expansion was reported in the previous literature for PNCs and was confirmed by peak shift in temperature dependent PL and shift in XRD peaks, it was not clearly observed in this measurement.

TABLE I. d-spacing of 6 different PNC_{35_APTMS} at 96 K and 300 K.

Particle	d-spacing at 96 K	d-spacing at 300 K
No. 1	0.29	0.29
No. 2	0.29	0.29
No. 3	0.29	0.28
No. 4	0.29	0.28
No. 5	0.30	0.29
No. 6	0.28	0.28
Average	0.29	0.29

IV. CONCLUSION

In summary, the optical and structural properties of three different sized PNCs have been studied as a function of temperature. The small PNCs (PNC_{50_APTMS}) showed a slight blue shift in the PL spectra with lowering temperature, which is opposite to that observed for large- and middle-sized PNCs. This blue shift at low temperatures was previously suggested to be an indication of phase transition from tetragonal to orthorhombic crystal structures; however, our experimental data overruled that. The PL lifetime of larger PNCs increased dramatically with temperature, which is attributed to the exciton splitting to free carriers at higher temperatures and the formation of polar domains in the PNCs. Interestingly, the small and middle-sized PNCs showed no significant change in lifetime with lowering temperature, opposite to the trend observed for large PNCs. This is attributed to the proper surface passivation of small and middle-sized PNCs with higher concentration of passivating ligand (APTMS) and lower density of surface trap states. In addition, the charge carrier delocalization can be controlled by varying the size of the PNCs. The cryo-XRD data did not show evidence of phase transition, suggesting efficient crystal phase stabilization with varying concentrations of APTMS and different PNC sizes.

ACKNOWLEDGMENTS

This project was supported by NASA through the MACES Center at UC Merced (Grant No. NNX15AQ01A), the National Science Foundation (Grant No. CHE 1906711), and the UCSC Senate Special Research Fund. Work at the Molecular Foundry was supported by the Office of Science, Office of Basic Energy Sciences, the U.S. Department of Energy under Contract No. DE-AC02-05CH11231. We would also like to acknowledge the work of Jesse Hauser of the

Scott Oliver lab (University of California Santa Cruz) for collecting XRD data using a Rigaku SmartLab X-ray diffractometer funded by the NSF Major Research Instrument (MRI) Program under Grant No. DMR-1126845.

REFERENCES

[1]H.-S. Kim, C.-R. Lee, J.-H. Im, K.-B. Lee, T. Moehl, A. Marchioro, S.-J. Moon, R. Humphry-Baker, J.-H. Yum, J. E. Moser *et al.*, "Lead iodide perovskite sensitized all-solid-state submicron thin film mesoscopic solar cell with efficiency exceeding 9%," Sci. Rep. **2**, 591 (2012).

[2]W. S. Yang, J. H. Noh, N. J. Jeon, Y. C. Kim, S. Ryu, J. Seo, and S. I. Seok, "High-performance photovoltaic perovskite layers fabricated through intramolecular exchange," Science **348**(6240), 1234–1237 (2015).

[3]Q. Dong, Y. Fang, Y. Shao, P. Mulligan, J. Qiu, L. Cao, and J. Huang, "Electron-hole diffusion lengths; 175 Mm in solution-grown $CH_3NH_3PbI_3$ single crystals," Science **347**(6225), 967–970 (2015).

[4]H. Cho, S.-H. Jeong, M.-H. Park, Y.-H. Kim, C. Wolf, C.-L. Lee, J. H. Heo, A. Sadhanala, N. Myoung, S. Yoo *et al.*, "Overcoming the electroluminescence efficiency limitations of perovskite light-emitting diodes," Science **350**(6265), 1222–1225 (2015).

[5]Z.-K. Tan, R. S. Moghaddam, M. L. Lai, P. Docampo, R. Higler, F. Deschler, M. Price, A. Sadhanala, L. M. Pazos, D. Credgington *et al.*, "Bright light-emitting diodes based on organometal halide perovskite," Nat. Nanotechnol. **9**(9), 687–692 (2014).

[6]S. A. Veldhuis, P. P. Boix, N. Yantara, M. Li, T. C. Sum, N. Mathews, and S. G. Mhaisalkar, "Perovskite materials for light-emitting diodes and lasers," Adv. Mater. **28**(32), 6804–6834 (2016).

[7]G. Xing, N. Mathews, S. S. Lim, N. Yantara, X. Liu, D. Sabba, M. Grätzel, S. Mhaisalkar, and T. C. Sum, "Low-temperature solution-processed wavelength-tunable perovskites for lasing," Nat. Mater. **13**(5), 476–480 (2014).

[8]H. Zhu, Y. Fu, F. Meng, X. Wu, Z. Gong, Q. Ding, M. V. Gustafsson, M. T. Trinh, S. Jin, and X.-Y. Zhu, "Lead halide perovskite nanowire lasers with low lasing thresholds and high quality factors," Nat. Mater. **14**(6), 636–642 (2015).

[9]X. Zheng, C. Wu, S. K. Jha, Z. Li, K. Zhu, and S. Priya, "Improved phase stability of formamidinium lead triiodide perovskite by strain relaxation," ACS Energy Lett. **1**(5), 1014–1020 (2016).

[10]B. T. Diroll, H. Zhou, and R. D. Schaller, "Low-temperature absorption, photoluminescence, and lifetime of $CsPbX_3$ (X = Cl, Br, I) nanocrystals," Adv. Funct. Mater. **28**(30), 1800945 (2018).

[11]S. Yakunin, L. Protesescu, F. Krieg, M. I. Bodnarchuk, G. Nedelcu, M. Humer, G. De Luca, M. Fiebig, W. Heiss, and M. V. Kovalenko, "Low-threshold amplified spontaneous emission and lasing from colloidal nanocrystals of caesium lead halide perovskites," Nat. Commun. **6**, 8056 (2015).

[12]S. B. Naghadeh, B. Luo, Y.-C. Pu, Z. Schwartz, W. R. Hollingsworth, S. A. Lindley, A. S. Brewer, A. L. Ayzner, and J. Z. Zhang, "Size dependence of charge carrier dynamics in organometal halide perovskite nanocrystals: Deciphering radiative versus nonradiative components," J. Phys. Chem. C **123**(7), 4610–4619 (2019).

[13]S. Sarang, H. Ishihara, Y.-C. Chen, O. Lin, A. Gopinathan, V. C. Tung, and S. Ghosh, "Low temperature excitonic spectroscopy and dynamics as a probe of quality in hybrid perovskite thin films," Phys. Chem. Chem. Phys. **18**(41), 28428–28433 (2016).

[14]J. Li, X. Yuan, P. Jing, J. Li, M. Wei, J. Hua, J. Zhao, and L. Tian, "Temperature-dependent photoluminescence of inorganic perovskite nanocrystal films," RSC Adv. **6**(82), 78311–78316 (2016).

[15]S. Sarang, S. Bonabi Naghadeh, B. Luo, P. Kumar, E. Betady, V. Tung, M. Scheibner, J. Z. Zhang, and S. Ghosh, "Stabilization of the cubic crystalline phase in organometal halide perovskite quantum dots via surface energy manipulation," J. Phys. Chem. Lett. **8**(21), 5378–5384 (2017).

[16]B. Luo, Y.-C. Pu, S. A. Lindley, Y. Yang, L. Lu, Y. Li, X. Li, and J. Z. Zhang, "Organolead halide perovskite nanocrystals: Branched capping ligands control crystal size and stability," Angew. Chem., Int. Ed. **55**(31), 8864–8868 (2016).

[17]K.-F. Lin, H.-M. Cheng, H.-C. Hsu, L.-J. Lin, and W.-F. Hsieh, "Band gap variation of size-controlled ZnO quantum dots synthesized by sol–gel method," Chem. Phys. Lett. **409**(4), 208–211 (2005).

[18]T. S. Kondratenko, M. S. Smirnov, O. V. Ovchinnikov, E. V. Shabunya-Klyachkovskaya, A. S. Matsukovich, A. I. Zvyagin, and Y. A. Vinokur, "Size-dependent optical properties of colloidal CdS quantum dots passivated by thioglycolic acid," Semiconductors **52**(9), 1137–1144 (2018).

[19]L. E. Brus, "Electron–electron and electron–hole interactions in small semiconductor crystallites: The size dependence of the lowest excited electronic state," J. Chem. Phys. **80**(9), 4403–4409 (1984).

[20]A. Henglein, "Small-particle research: Physicochemical properties of extremely small colloidal metal and semiconductor particles," Chem. Rev. **89**(8), 1861–1873 (1989).

[21]A. I. Ekimov, F. Hache, M. C. Schanne-Klein, D. Ricard, C. Flytzanis, I. A. Kudryavtsev, T. V. Yazeva, A. V. Rodina, and A. L. Efros, "Absorption and intensity-dependent photoluminescence measurements on CdSe quantum dots: Assignment of the first electronic transitions," J. Opt. Soc. Am. B **10**(1), 100–107 (1993).

[22]M. C. Brennan, J. E. Herr, T. S. Nguyen-Beck, J. Zinna, S. Draguta, S. Rouvimov, J. Parkhill, and M. Kuno, "Origin of the size-dependent Stokes shift in $CsPbBr_3$ perovskite nanocrystals," J. Am. Chem. Soc. **139**(35), 12201–12208 (2017).

[23]P. C. Sercel, J. L. Lyons, D. Wickramaratne, R. Vaxenburg, N. Bernstein, and A. L. Efros, "Exciton fine structure in perovskite nanocrystals," Nano Lett. **19**(6), 4068–4077 (2019).

[24]M. A. Becker, R. Vaxenburg, G. Nedelcu, P. C. Sercel, A. Shabaev, M. J. Mehl, J. G. Michopoulos, S. G. Lambrakos, N. Bernstein, J. L. Lyons *et al.*, "Bright triplet excitons in caesium lead halide perovskites," Nature **553**(7687), 189–193 (2018).

[25]K.-H. Wang, L.-C. Li, M. Shellaiah, and K. W. Sun, "Structural and photophysical properties of methylammonium lead tribromide ($MAPbBr_3$) single crystals," Sci. Rep. **7**(1), 13643 (2017).

[26]W. Kong, Z. Ye, Z. Qi, B. Zhang, M. Wang, A. Rahimi-Iman, and H. Wu, "Characterization of an abnormal photoluminescence behavior upon crystal-phase transition of perovskite $CH_3NH_3PbI_3$," Phys. Chem. Chem. Phys. **17**(25), 16405–16411 (2015).

[27]A. Francisco-López, B. Charles, O. J. Weber, M. I. Alonso, M. Garriga, M. Campoy-Quiles, M. T. Weller, and A. R. Goñi, "Equal footing of thermal expansion and electron–phonon interaction in the temperature dependence of lead halide perovskite band gaps," J. Phys. Chem. Lett. **10**, 2971–2977 (2019).

[28]M. Cui, Z. Zhang, Y. Wang, A. Finch, and P. D. Townsend, "Temperature dependence of bulk luminescence from ZnO," Luminescence **33**(4), 654–659 (2018).

[29]R. K. Misra, S. Aharon, B. Li, D. Mogilyansky, I. Visoly-Fisher, L. Etgar, and E. A. Katz, "Temperature- and component-dependent degradation of perovskite photovoltaic materials under concentrated sunlight," J. Phys. Chem. Lett. **6**(3), 326–330 (2015).

[30]W.-J. Yin, J.-H. Yang, J. Kang, Y. Yan, and S.-H. Wei, "Halide perovskite materials for solar cells: A theoretical review," J. Mater. Chem. A **3**(17), 8926–8942 (2015).

[31]Y. P. Varshni, "Temperature dependence of the energy gap in semiconductors," Physica **34**(1), 149–154 (1967).

[32]Z. Wan-Ru, G.-E. Weng, L. Ming-Ming, L. Zeng-Cheng, L. Jian-Ping, Z. Jiang-Yong, and Z. Bao-Ping, "Temperature dependence of emission properties of self-assembled InGaN quantum dots," Chin. Phys. Lett. **31**, 114205 (2014).

[33]C. Chen, X. Hu, W. Lu, S. Chang, L. Shi, L. Li, H. Zhong, and J.-B. Han, "Elucidating the phase transitions and temperature-dependent photoluminescence of $MAPbBr_3$ single crystal," J. Phys. Appl. Phys. **51**(4), 045105 (2018).

[34]P. S. Whitfield, N. Herron, W. E. Guise, K. Page, Y. Q. Cheng, I. Milas, and M. K. Crawford, "Structures, phase transitions and tricritical behavior of the hybrid perovskite methyl ammonium lead iodide," Sci. Rep. **6**(1), 35685 (2016).

[35]R. Saran, A. Heuer-Jungemann, A. G. Kanaras, and R. J. Curry, "Giant bandgap renormalization and exciton–phonon scattering in perovskite nanocrystals," Adv. Opt. Mater. **5**(17), 1700231 (2017).

[36]R. L. Milot, G. E. Eperon, H. J. Snaith, M. B. Johnston, and L. M. Herz, "Temperature-dependent charge-carrier dynamics in $CH_3NH_3PbI_3$ perovskite thin films," Adv. Funct. Mater. **25**(39), 6218–6227 (2015).
[37]H.-H. Fang, F. Wang, S. Adjokatse, N. Zhao, J. Even, and M. Antonietta Loi, "Photoexcitation dynamics in solution-processed formamidinium lead iodide perovskite thin films for solar cell applications," Light Sci. Appl. **5**(4), e16056 (2016).
[38]K. Wei, Z. Xu, R. Chen, X. Zheng, X. Cheng, and T. Jiang, "Temperature-dependent excitonic photoluminescence excited by two-photon absorption in perovskite $CsPbBr_3$ quantum dots," Opt. Lett. **41**(16), 3821–3824 (2016).
[39]B. T. Diroll, G. Nedelcu, M. V. Kovalenko, and R. D. Schaller, "High-temperature photoluminescence of $CsPbX_3$ (X = Cl, Br, I) nanocrystals," Adv. Funct. Mater. **27**(21), 1606750 (2017).
[40]L. C. Schmidt, A. Pertegás, S. González-Carrero, O. Malinkiewicz, S. Agouram, G. Mínguez Espallargas, H. J. Bolink, R. E. Galian, and J. Pérez-Prieto, "Nontemplate synthesis of $CH_3NH_3PbBr_3$ perovskite nanoparticles," J. Am. Chem. Soc. **136**(3), 850–853 (2014).
[41]X. Chen, J. Jiang, F. Yan, S. Tian, and K. Li, "A novel low temperature vapor phase hydrolysis method for the production of nano-structured silica materials using silicon tetrachloride," RSC Adv. **4**(17), 8703–8710 (2014).